Received: 7 March 2024 | Revised: 13 May 2024 | Accepted: 29 May 2024

DOI: 10.1002/alz.14095

Alzheimer's & Dementia®
THE JOURNAL OF THE ALZHEIMER'S ASSOCIATION

RESEARCH ARTICLE

Omics-derived biological modules reflect metabolic brain changes in Alzheimer's disease

Guilherme Povala[1,2,3] | Marco Antônio De Bastiani[1] | Bruna Bellaver[1,3] | Pamela C. L. Ferreira[3] | João Pedro Ferrari-Souza[1] | Firoza Z. Lussier[3] | Diogo O. Souza[1,4] | Pedro Rosa-Neto[5] | Tharick A. Pascoal[3,6] | Bruno Zatt[2] | Eduardo R. Zimmer[1,7,8,9] | for the Alzheimer's Disease Neuroimaging Initiative

[1]Graduate Program in Biological Sciences: Biochemistry, Universidade Federal do Rio Grande do Sul (UFRGS), Porto Alegre, Brazil

[2]Graduate Program in Computing, Universidade Federal de Pelotas (UFPEL), Porto Alegre, Brazil

[3]Department of Psychiatry, School of Medicine, University of Pittsburgh, Pittsburgh, Pennsylvania, USA

[4]Department of Biochemistry, Universidade Federal do Rio Grande do Sul (UFRGS), Porto Alegre, Brazil

[5]Translational Neuroimaging Laboratory, The McGill University Research Centre for Studies in Aging, Montreal, Quebec, Canada

[6]Department of Neurology, School of Medicine, University of Pittsburgh, Pittsburgh, Pennsylvania, USA

[7]Department of Pharmacology, Universidade Federal do Rio Grande do Sul (UFRGS), Porto Alegre, Brazil

[8]Graduate Program in Biological Sciences: Pharmacology and Therapeutics, Universidade Federal do Rio Grande do Sul (UFRGS), Porto Alegre, Brazil

[9]Brain Institute of Rio Grande do Sul, Pontifícia Universidade Católica do Rio Grande do Sul, Porto Alegre, Brazil

Correspondence
Eduardo R. Zimmer, Department of Pharmacology, Universidade Federal do Rio Grande do Sul (UFRGS), 2500 Ramiro Barcelos Street, 90035-003, Porto Alegre, Rio Grande do Sul, Brazil.
Email: erzimmer@gmail.com

Funding information
Alzheimer's Association, Grant/Award Numbers: #24AARFD-1243899, #AARFD-23-1148735, #AARFD-22-974627, #AARFD-22-974627, #NIRG-12-92090, AARGD-21-850670; CNPq, Grant/Award Numbers: #150512/2022-8, 435642/2018-9, 312410/2018-2, 409066/2022-2, 312306/2021-0, 409595/2023-3; Weston Brain Institute; Canadian Institutes of Health Research, Grant/Award Numbers: #MOP-11-51-31, RFN 152985, 159815, 162303; Canadian Consortium of Neurodegeneration and Aging, Grant/Award Number: MOP-11-51-31-team 1; Brain Canada Foundation, Grant/Award Numbers:

Abstract

INTRODUCTION: Brain glucose hypometabolism, indexed by the fluorodeoxyglucose positron emission tomography ([^{18}F]FDG-PET) imaging, is a metabolic signature of Alzheimer's disease (AD). However, the underlying biological pathways involved in these metabolic changes remain elusive.

METHODS: Here, we integrated [^{18}F]FDG-PET images with blood and hippocampal transcriptomic data from cognitively unimpaired (CU, n = 445) and cognitively impaired (CI, n = 749) individuals using modular dimension reduction techniques and voxel-wise linear regression analysis.

RESULTS: Our results showed that multiple transcriptomic modules are associated with brain [^{18}F]FDG-PET metabolism, with the top hits being a protein serine/threonine kinase activity gene cluster (peak-$t_{(223)}$ = 4.86, P value < 0.001) and zinc-finger–related regulatory units (peak-$t_{(223)}$ = 3.90, P value < 0.001).

DISCUSSION: By integrating transcriptomics with PET imaging data, we identified that serine/threonine kinase activity–associated genes and zinc-finger–related regulatory units are highly associated with brain metabolic changes in AD.

Guilherme Povala and Marco Antônio De Bastiani contributed equally to this work.

34874, 33397; Fonds de Recherche du Québec – Santé (Chercheur Boursier, Grant/Award Number: #2020-VICO-279314; National Institute on Aging, Grant/Award Numbers: R01AG075336, R01AG073267; CAPES, Grant/Award Number: #88887.627297/2021-00; Instituto Serrapilheira, Grant/Award Number: #Serra-1912-31365; Brazilian National Institute of Science and Technology in Excitotoxicity and Neuroprotection, Grant/Award Number: #465671/2014-4; ARD/FAPERGS, Grant/Award Number: #21/2551-0000673-0; Alzheimer's Association and Natinal Academy of Neuropsychology, Grant/Award Number: ALZ-NAN-22-928381

KEYWORDS
Alzheimer's disease, fluorodeoxyglucose positron emission tomography, systems biology, transcriptomics

Highlights

- We conducted an integrated analysis of system-based transcriptomics and fluorodeoxyglucose positron emission tomography ([^{18}F]FDG-PET) at the voxel level in Alzheimer's disease (AD).
- The biological process of serine/threonine kinase activity was the most associated with [^{18}F]FDG-PET in the AD brain.
- Serine/threonine kinase activity alterations are associated with brain vulnerable regions in AD [^{18}F]FDG-PET.
- Zinc-finger transcription factor targets were associated with AD brain [^{18}F]FDG-PET metabolism.

1 | BACKGROUND

Alzheimer's disease (AD) is the most prevalent neurodegenerative disease affecting the elderly.[1] In recent decades, a vital concept shift has led to AD being recognized as a clinical–biological entity. In this context, positron emission tomography (PET) currently allows for visualizing AD pathophysiological changes in living individuals.[2] Indeed, these technologies have contributed to an improved understanding of AD and boosted a new era of enormous imaging data collection in multiple centers worldwide and collaborative initiatives.

The most used PET radiopharmaceutical in neurodegenerative disorders is the glucose analog [^{18}F]Fluorodeoxyglucose (FDG). A typical signature of [^{18}F]FDG-PET hypometabolism is seen in the brain of AD individuals.[3] This glucose hypometabolism has been interpreted as a marker of neurodegeneration in AD.[4,5] Studies have shown that its biological interpretation is much more complex, involving interactions of different brain cell types. More specifically, neurons, astrocytes, and microglial cells contribute to the [^{18}F]FDG-PET signal and are now acknowledged in their biological interpretation.[4,6–8] However, the biological pathways involved in AD-related [^{18}F]FDG-PET hypometabolism remain unclear.

There has been an increasing call for multimodal imaging studies associated with refined integrative and network strategies.[9,10] Indeed, integrating PET with omics technologies is one strategy to advance our understanding of biological features associated with [^{18}F]FDG-PET hypometabolism in AD. Transcriptomics is particularly attractive because RNAs represent an intermediate level between the static genomics context and the spatiotemporal dynamic of proteomics complexity.[11] In this regard, systems biology methods can be instrumental in unraveling novel features.[12] Neuroimaging data integration in recent years has focused on the gene level,[13,14] but genes rarely dictate phenotypes alone; they act in concert to modulate phenotypic transitions.

With this in mind, we sought to implement two systems-based strategies to uncover biological modules associated with brain glucose metabolism changes in AD. We hypothesized that modular approaches based on groups of genes would yield better associations with higher-order biological manifestations and may uncover novel biological features of AD.

2 | METHODS

2.1 | Study participants

We used data from the multicenter Alzheimer's Disease Neuroimaging Initiative (ADNI) study, available at http://adni.loni.usc.edu/. This study is designed to develop and validate neuroimaging and biomarkers for the early detection, monitoring, and treatment of AD. Further details regarding its inclusion criteria have been described elsewhere.[15] Our study included all participants with available blood microarray data. Additionally, a subset of these participants also had [^{18}F]FDG-PET brain imaging available. According to diagnostic criteria defined in ADNI,[16] individuals without significant cognitive impairment or impact on daily living activities were classified as cognitively unimpaired (CU). This group comprised individuals with a Mini-Mental State Examination (MMSE) score ranging from 24 to 30, a Clinical Dementia Rating (CDR) of 0, and a Memory Box score of 0. Participants diagnosed with mild cognitive impairment (MCI) or dementia were categorized as cognitively impaired (CI). This CI group included individuals with an MMSE score between 24 and 30, a CDR of 0.5, and a Memory Box score of at least 0.5. In these cases, general cognition and functional performance were sufficiently preserved to preclude an AD diagnosis at the screening visit. Additionally, individuals with an MMSE score between 20 and 26 and a CDR $\geq$ 0.5, meeting the National Institute of Neurological and Communicative Disorders and Stroke/Alzheimer's

Disease and Related Disorders Association criteria for probable AD, were also included in this group. More details about the group inclusion criteria and exceptions can be found in the ADNI Procedures Manual.[16]

2.2 | Blood expression data acquisition

We obtained blood microarray data from ADNI, including only samples with RNA integrity scores > 7. After RNA integrity and quality control filters, the resulting ADNI dataset retained 317 samples (218 CI and 99 CU individuals). We also obtained additional processed blood microarray datasets from the Gene Expression Omnibus (GEO) repository (https://www.ncbi.nlm.nih.gov/geo/; Figure 1A) using the GEOquery package (v2.56.0).[17] From GEO, we obtained data from GSE63063,[18] which contains 433 CI and 223 CU samples from the AddNeuroMed Cohort, and from GSE97760,[19] with 8 CI and 7 CU individuals.

Additionally, healthy human blood samples from two large microarray datasets were obtained from the GEO repository, GSE48348[20] and GSE99039.[21] These datasets were intersected under common gene symbol annotation using the virtualArray package (v1.8.0).[22] The resulting dataset retained 967 healthy blood samples used for transcriptional network inference.

2.3 | Brain expression data acquisition

Human AD hippocampal microarray data from six studies were obtained from GEO repository (GSE5281,[23] GSE28146,[24] GSE29378,[25] GSE36980,[26] GSE48350,[27] and GSE84422[28]), downloaded using the GEOquery package (v2.56.0)[17] and combined under common gene symbol annotations using the virtualArray package (v1.8.0;[22] Figure 1A). We processed raw data using the affy (v1.70.0)[29] and the vsn package.[30] Afterward, we applied a batch correction using the sva package.[31]

2.4 | Differential expression analyses

Differential expression analysis comparing CU versus CI was conducted on microarray data using the limma package (v3.48.3)[32] lmFit function to fit multiple linear models by generalized least squares. In addition, the eBayes function was used to compute moderated *t* statistics, moderated *F* statistics, and log-odds of differential expression by empirical Bayes moderation of the standard errors toward a common value (Figure 1B).

Due to high variability in blood transcriptomics and seeking consistency between datasets, only genes with a *P* value < 0.05 in at least two of three datasets were considered differentially expressed genes (DEGs) for blood samples. For brain samples, genes with false discovery rate–adjusted *P* value < 0.01 from the merged dataset were considered DEGs. We obtained the final list of genes used for further analyses from the intersection between blood and brain DEGs. Venn diagrams were constructed using the VennDiagram package (v1.6.20).[33]

RESEARCH IN CONTEXT

1. **Systematic review**: The authors reviewed the literature using PubMed and Web of Science and cited relevant studies. A few neuroimaging integration studies focused on associations between fluorodeoxyglucose positron emission tomography (FDG-PET) and gene-level alterations in Alzheimer's disease (AD). However, studies integrating FDG-PET and genetic information using a systems biology approach have not been addressed yet.
2. **Interpretation**: This study applies a modular-oriented transcriptomic approach integrated with neuroimaging to leverage new insights on AD pathology. Our findings highlight an association between serine/threonine kinase activity–related processes and regulatory units with [^{18}F]FDG-PET metabolism in the brains of individuals across the AD clinical spectrum.
3. **Future directions**: Future studies should validate the biological involvement of the gene modules observed here experimentally and use this novel integration method with other PET imaging tracers (e.g., amyloid beta PET, tau PET, translocator protein PET). This will lead to a better understanding of AD pathology and may contribute to improved diagnosis and therapeutics.

2.5 | Functional enrichment analyses and Gene Ontology semantic similarity

We used DEGs found in both blood and brain datasets for conducting Gene Ontology (GO) functional enrichment analysis. This analysis was carried out using the enrichGO function from the clusterProfiler package (v4.0.5).[34] This function uses an over-representation analysis method to ascertain if known biological functions or processes are significantly enriched within a gene list derived from experimental data.

Furthermore, we clustered the GO biological process terms by semantic similarity using the mgoSim function from the GOSemSim (v2.18.1) package[35] (arguments measure = "Wang" and combine = NULL). Semantic comparisons of GO annotations provide quantitative ways to compute similarities between genes and gene groups. We represented the resulting similarity matrices as GO networks using the RedeR (v1.40.0) package[36] for interactive visualization and manipulation of nested networks. We retained only similarity scores above the 80th percentile of score distribution for building the network. We manually named clusters of GO terms obtained from the GOSemSim algorithm for their biological interpretation (Figure 1C).

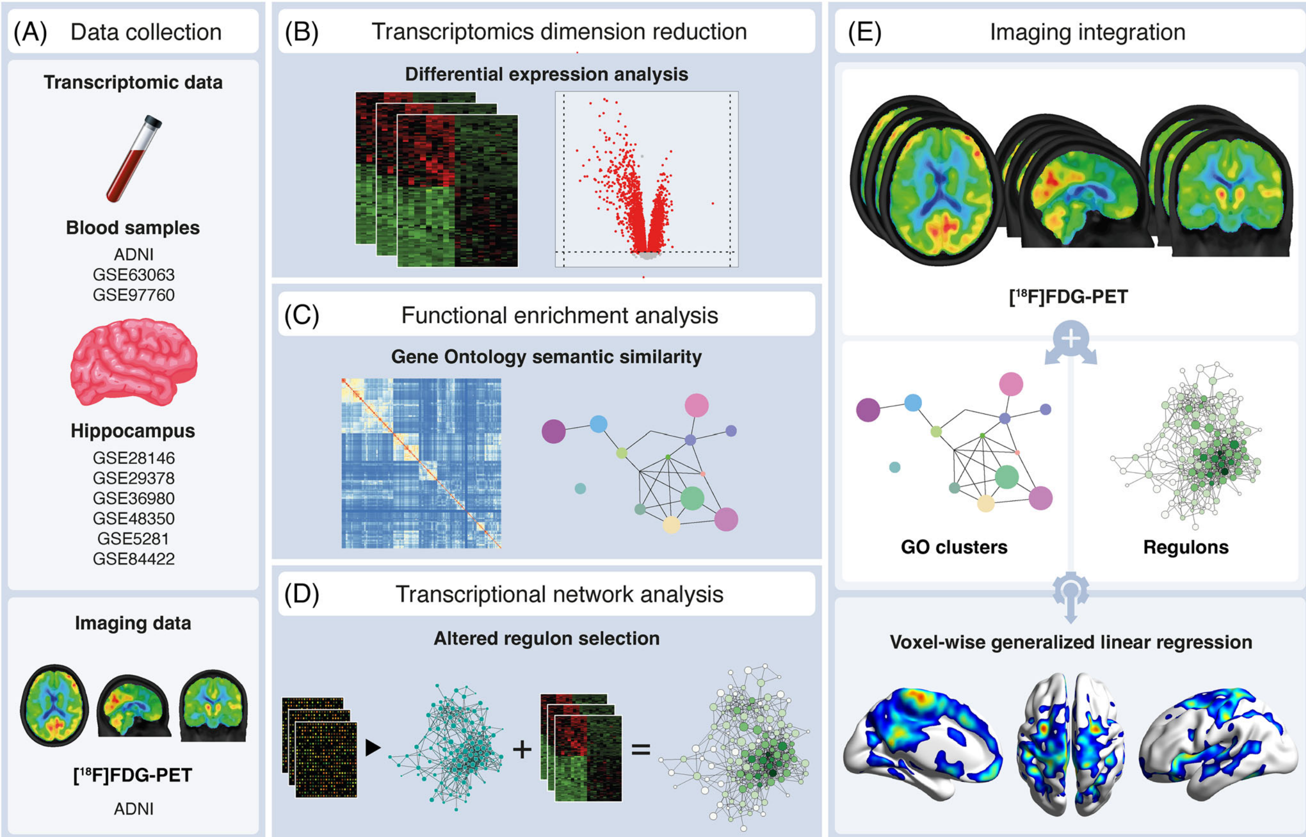

FIGURE 1 Omics-imaging integration pipeline. A, Data collection of blood and hippocampus samples and imaging data from multiple datasets. B, Transcriptomics dimension reduction using differential expression analysis. C, Functional enrichment analysis using the GO semantic similarity. D, Transcriptional network analysis, responsible for selecting altered regulatory units. E, Imaging integration using voxel-wise generalized linear regression between PET images and statistically altered GO clusters and regulatory units. ADNI, Alzheimer's Disease Neuroimaging Initiative; [^{18}F]FDG, fluorodeoxyglucose; GO, Gene Ontology; PET, positron emission tomography.

2.6 | Reverse engineering of transcriptional network and master regulator analysis

We identified master regulators among transcription factors (TFs) based on predictive and inferential modeling approaches. These models predict potential master regulators by analyzing large-scale gene expression data and inferring regulatory relationships. These methods use algorithms that evaluate the impact of specific transcription factors on the expression patterns of their target genes, allowing for the prediction of their regulatory influence within cellular networks.[37–41]

First, we inferred the transcriptional networks centered on transcription factors and their predicted target genes using a large cohort of healthy blood samples from publicly available datasets as described in Section 2.2. Herein, we used "regulatory unit" to describe the groups of inferred genes and their associated TFs. We used the RTN (v2.16.1) package to reconstruct and analyze transcriptional networks based on mutual information using the Algorithm for the Reconstruction of Accurate Cellular Networks (ARACNe) method.[37–39,42] In summary, the regulatory structure of the network is derived by mapping significant associations between known TFs and all potential targets. A curated list of genes obtained from Lambert et al.[40] was used to annotate TF eligibility for transcriptional network inference input. To create a consensus bootstrap network, we eliminated the interactions below a minimum mutual information threshold by a permutation step and removed unstable interactions by bootstrap. Finally, the data processing inequality algorithm is applied with null tolerance to eliminate interactions likely to be mediated by a third TF. The reference blood transcriptional network was built using the package's default number of 5000 permutations and 100 bootstraps (P value < 0.001).

Then, we conducted the master regulator analysis described by Carro et al.[43] on the regulatory units with $>$ 100 targets using the RTN (v2.16.1) package using the regulatory units identified in the previous step. For each regulatory unit in the blood transcriptional network, the algorithm computes the statistical overrepresentation (calculated by Fisher exact test) of genes obtained from differential expression analyses (P value < 0.05). Master regulator candidates altered in at least two thirds of the three case–control studies (ADNI, GSE63063, and GSE99039) were selected for gene set variation analysis and neuroimaging integration (Figure 1D).

2.7 | Gene set variation analysis

The enrichment scores obtained from the gene set variation analysis were used to collapse the activity of groups of genes into a single value for each sample.[44] This gene set enrichment method estimates group gene activity variation over a sample population in an unsupervised manner. Briefly, genes contained in the clusters of GO terms obtained from GOSemSim or in the regulatory units obtained from master regulator analysis were submitted to the gsva function (kcdf = "Gaussian") of the GSVA package in R.[44] We used the resulting enrichment score for further association with neuroimaging data and correlation analyses.

2.8 | Imaging pre-processing and integration

We acquired imaging data from the ADNI database (Figure 1A). [^{18}F]FDG-PET images were linearly registered to the T1-weighted image space. We linearly and non-linearly registered T1-weighted images to the Montreal Neurological Institute (MNI) template space. Subsequently, we performed an [^{18}F]FDG-PET non-linear registration using the linear and non-linear transformations from the T1-weighted image to the MNI space and the [^{18}F]FDG-PET to T1-weighted image registration. We performed these transformations using the *antsRegistrationSyNQuick* and *antsApplyTransforms* from advanced normalization tools (ANTs).[45] We spatially smoothed the [^{18}F]FDG-PET images to achieve a final resolution of 8 mm full width at half maximum using *mincblur* from MINC Tools (http://bic-mni.github.io/).

We created standardized uptake ratio maps of [^{18}F]FDG-PET using the cerebellum as the reference region. These images were then integrated with GO clusters and TF regulatory units using voxel-wise linear regression models, adjusting for age, sex, and years of education (Figure 1E). This analysis was performed using the RMINC software package (v1.5.2.1).[46] The voxel-wise correlations produced *t* statistical maps, and we included only those voxels that displayed statistically significant correlations, defined by a *P* value of 0.01, which corresponds to a *t* value of 2.6. To address the multiple comparisons in voxel-wise analysis, we applied the Bonferroni correction to adjust these thresholds, resulting in increased *t* value thresholds of 3.0 for integration with GO clusters and 3.4 for integration with TF regulatory units. Additionally, we extracted the percentage of significant voxels within each brain region from the *t* statistical maps, using the CerebrA ICBM152 atlas to define the regions of interest.[47,48]

3 | RESULTS

3.1 | Participants

We assessed 317 individuals from ADNI, including 99 CU and 218 CI individuals, who had available blood microarray data. The demographic and clinical characteristics of this population are detailed in Table 1. From ADNI, we also acquired [^{18}F]FDG-PET scans for 227 individuals, including 69 CU and 158 CI. From the GEO database, we included data from GSE63063, with 223 CU and 433 CI; GSE9776, with 7 CU and 8 CI; GSE48348, with 734 CU; and GSE99039, with 233 CU. Additionally, we combined human AD hippocampal microarray data from six studies, which included 116 CU and 90 CI individuals. The metadata for these datasets is presented in Table S1 in supporting information, and further demographic information is provided in Table S2 in supporting information.

TABLE 1 Demographics and key characteristics of participants from ADNI.

Characteristics	CU ($n = 99$)	CI ($n = 217$)
Age, mean (SD)	73.9 (5.84)	71.6 (7.22)
Sex, *n* (% female)	53 (53.5)	91 (41.9)
Years of education, mean (SD)	16.5 (2.73)	16.0 (2.79)
CDR sum of boxes (SD)	0.0670 (0.336)	2.30 (2.23)
MMSE (SD)	29.2 (0.952)	26.7 (3.48)

Abbreviations: ADNI, Alzheimer's Disease Neuroimaging Initiative; CDR, Clinical Dementia Rating; CI, cognitively impaired; CU, cognitively unimpaired; MMSE, Mini-Mental State Examination; SD, standard deviation.

3.2 | Dimension reduction analysis identifies key altered genes in AD

The novel dimension reduction strategy proposed in this study for analyzing transcriptomic data from blood and hippocampal samples is illustrated in Figure 2. Figure 2A details the gene counts after each step of the dimension reduction strategy. After merging datasets, we identified 16,126 genes in the blood and 10,845 genes in the hippocampus.

Using the gene expression data from each tissue, our differential expression analysis comparing CU and CI individuals revealed 2875 DEGs in the blood and 1979 DEGs in the hippocampus. Importantly, 428 DEGs were consistently altered in both tissues. Details about DEGs from datasets are shown in Tables S3 and S4 in supporting information.

3.3 | Functional enrichment and semantic similarity analysis highlight key altered biological processes in AD

After the identification of overlapped DEGs, we conducted a functional enrichment analysis to discern the GO biological processes implicated by these genes. This analysis identified 89 significantly enriched GO biological process terms (Table S5 in supporting information), highlighting alterations in critical processes such as oxidative phosphorylation in mitochondria and cell cycle, and response to stress, which are indicative of their potential roles in AD pathophysiology.

We subsequently applied a semantic similarity method to cluster the GO biological processes into similar functional relevance, resulting

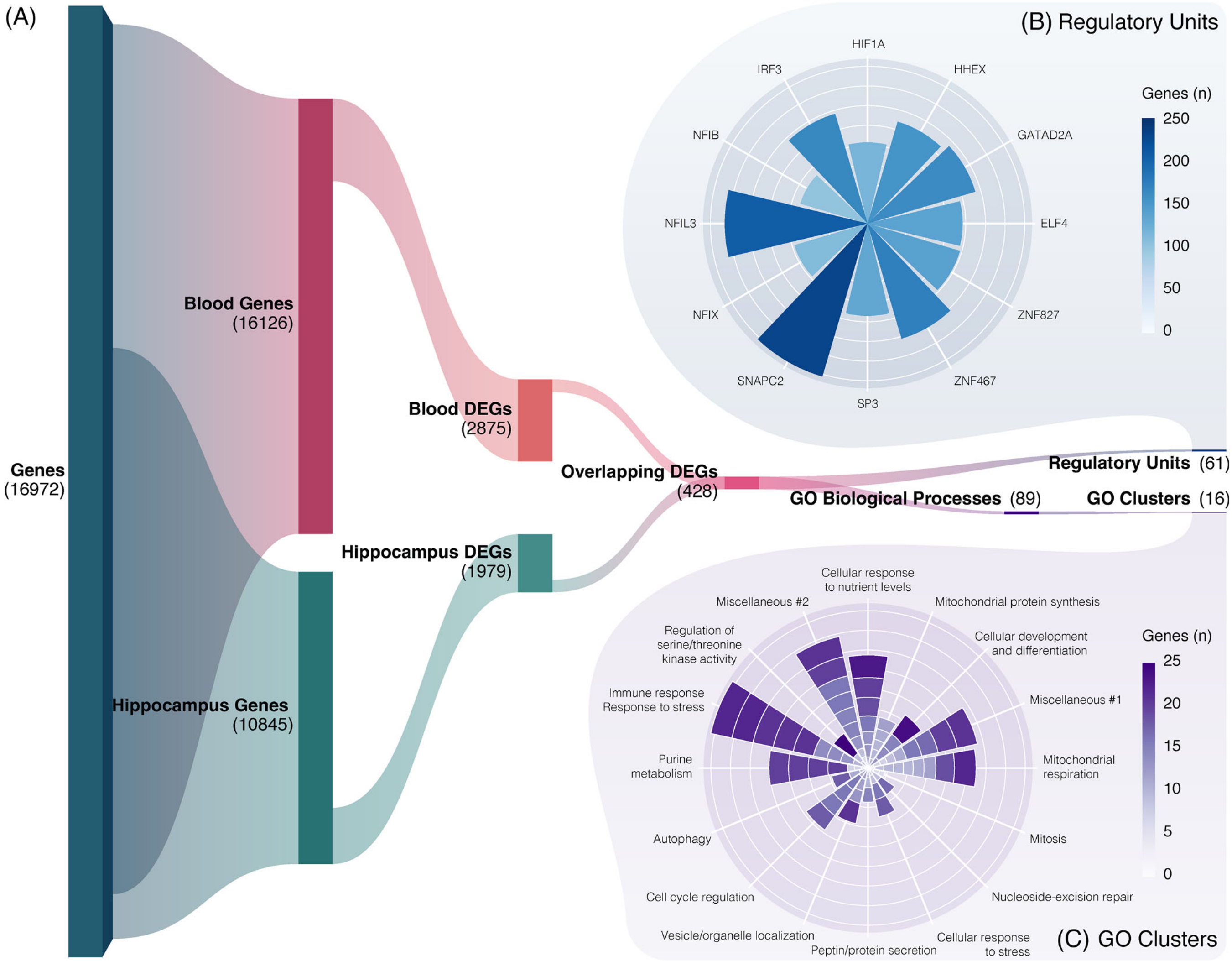

FIGURE 2 Sankey flow diagram representing the dimension reduction strategy. A, Transcriptomic data from blood and hippocampus cohorts underwent differential expression analysis between cognitively unimpaired and impaired individuals. Overlapping differentially expressed genes (DEGs) from both tissues were selected, and Gene Ontology (GO) biological processes were derived through functional enrichment analysis, with GO terms clustered based on semantic similarity to identify functionally relevant groups. Additionally, regulatory units of transcription factors were generated using the same overlapping DEGs. B, The sunburst plot of regulatory units displays the gene count for 12 units selected based on the enrichment score quartiles (10% and 90%). C, In the sunburst plot of GO clusters, each segment displays the gene count for individual GO terms within the cluster, acknowledging their composition of multiple GOs.

in 16 distinct GO clusters (Figure 2C). These GO clusters are visually represented in a network diagram (Figure 3). In the network, each node (cluster) is sized proportionally to the number of terms it contains, and the edges are weighted by the similarity scores, which reflect the degree of similarity between connected clusters (Table S6 in supporting information). Notably, the clusters related to "regulation of serine/threonine kinase activity" and "DNA repair and metabolism" exhibited the highest connectivity, suggesting their pivotal roles in AD pathophysiology. Figure S1 in supporting information shows the heatmap of the semantic similarity matrix based on the GO terms and the resulting clusters of terms. It is important to note that GO clusters #2 and #6, as referenced in Table S6, include a variety of biological processes that do not share common functions. Consequently, due to their varied nature, these clusters have been labeled "Miscellaneous" and are not included in further analyses.

3.4 | Transcriptional network analysis reveals key altered regulatory units in AD

We used reverse engineering of transcriptional networks to infer groups of regulatory units controlled by transcription factors. This method aimed to consolidate groups of altered genes into coherent biological modules. The master regulator analysis identified the regulatory units of TFs that were most enriched with DEGs. Specifically, we observed that 34, 92, and 41 regulatory units were statistically

Alzheimer's & Dementia®
THE JOURNAL OF THE ALZHEIMER'S ASSOCIATION

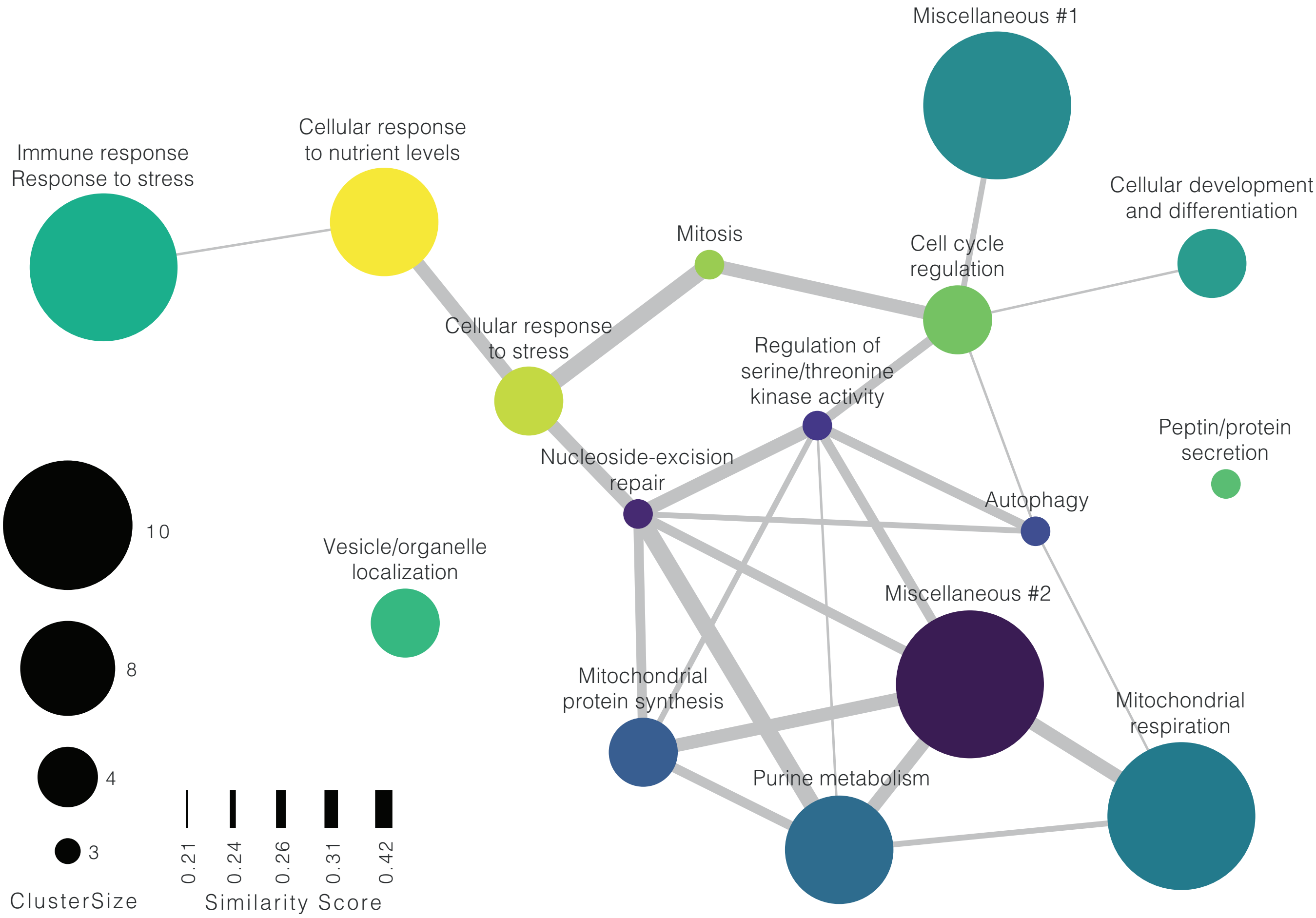

FIGURE 3 Gene Ontology (GO) semantic similarity network. GO biological process terms were clustered by semantic similarity and mapped to a network, with cluster sizes represented as nodes and cluster similarity coefficients as edges.

altered in the ADNI, GSE63063, and GSE97760 blood datasets, respectively (Table S7 in supporting information). Notably, 61 regulatory units were significantly enriched with DEGs across at least two of the three datasets analyzed, and 12 were consistently altered across all datasets (Figure 2B).

We performed gene set enrichment analyses that illustrate the phenotypic associations (CI vs. CU) of the top 10 altered regulatory units (Figure S2 in supporting information). Additionally, we evaluated the GO functional enrichment for each of these top 10 regulatory units (Table S8 in supporting information) and visualized the results in a network diagram shown in Figure 4. These results indicate that most regulatory units are associated with altered biological processes. However, the regulatory units for GATA1 and ZNF358, for example, contained mixed element types and were predominantly related to cellular component terms. Interestingly, the ZNF653 regulatory unit showed stronger connections with GO terms related to energy metabolism and protein kinase activity. Of note, no significant enrichment of GO terms was observed for the ZZZ3 regulatory unit.

3.5 | Voxel-wise analysis identifies significant associations between gene clusters and brain metabolism in AD

Using the 16 GO clusters obtained from semantic similarity analysis, we performed voxel-wise analysis to identify the topographical associations between [^{18}F]FDG-PET metabolism and GO cluster enrichment scores. Of the 16 GO clusters, the cluster involved in the regulation of protein serine/threonine kinase activity showed the most significant associations with brain metabolism (peak t value = 4.86, P value < 0.001; Figure 5A). Furthermore, the association of this cluster with brain metabolic signals was particularly prominent in regions highly vulnerable to AD. Specifically, in the precuneus' gray matter, 59.25% of the voxels in the left hemisphere and 68.63% of the right hemisphere showed significant associations; in the medial frontal gyrus, 52.76% of left and 14.01% of right voxels; in the medial frontal–orbital gyrus, 51.39% of left and 11.58% of right voxels; and in the cingulate region, 46.60% of left and 18.46% of right voxels demonstrated significant correlations (Figure 5B).

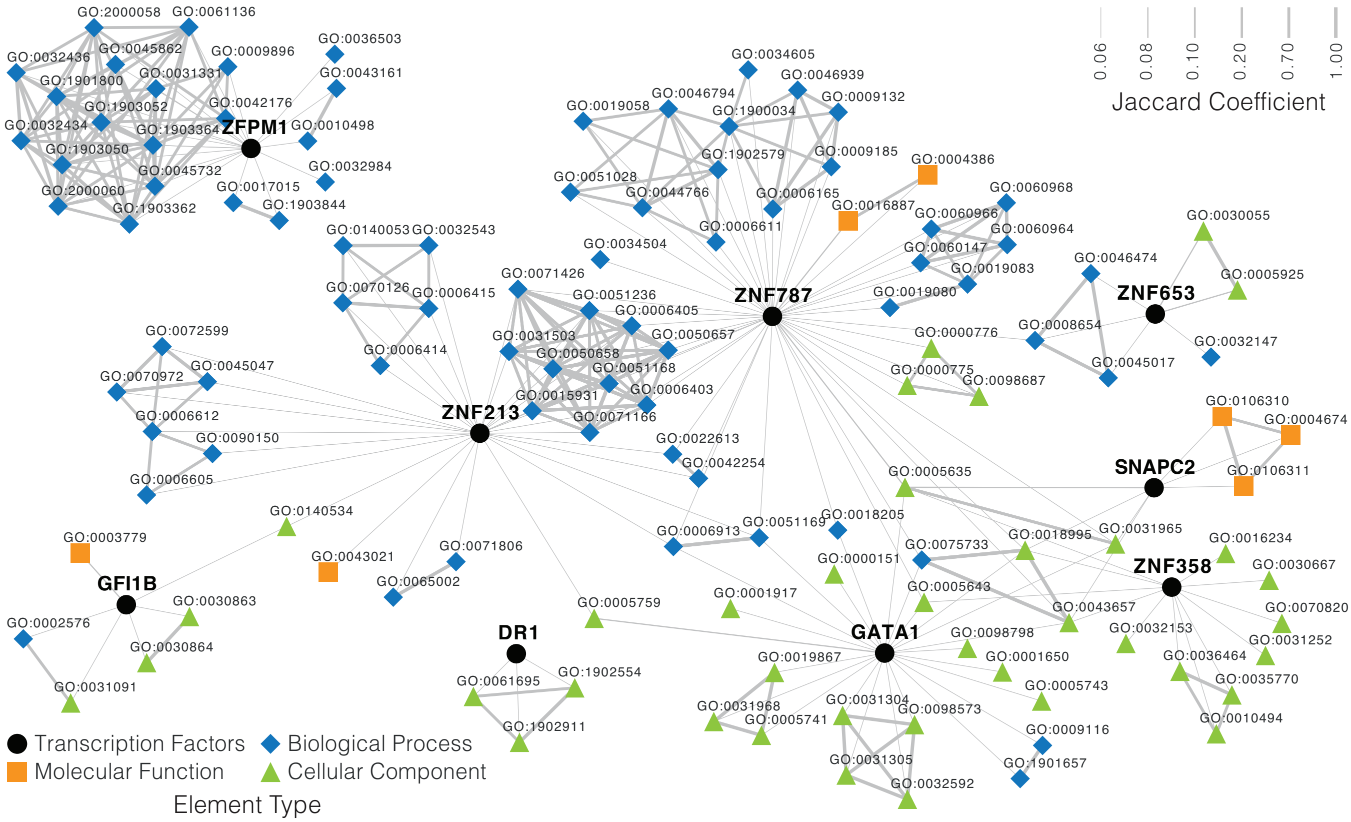

FIGURE 4 Gene Ontology (GO) functional enrichment of regulatory units. The top 10 altered regulatory units were evaluated for GO functional enrichment and mapped to a network, with node shapes representing different elements and with edges representing the gene overlap between GO terms (Jaccard coefficient).

Similarly, we conducted voxel-wise linear regressions to investigate the spatial associations between [^{18}F]FDG-PET signals and the regulatory units enriched with DEGs. Among the 61 regulatory units, ZNF653 was most closely associated with brain glucose metabolism (peak t value = 3.90, P value < 0.001; Figure 5C). This association was also most prominent in regions vulnerable to AD. For instance, in the precuneus' gray matter, significant associations were observed in 24.24% of the voxels in the left hemisphere and 39.51% of the right voxels; in the medial frontal gyrus, 17.26% of left voxels; in the medial frontal-orbital gyrus, 12.50% of left voxels; and in the precentral gyrus, 9.08% of left and 8.28% of right voxels showed significant correlations (Figure 5D).

4 | DISCUSSION

In the present study, we identified novel biological features associated with [^{18}F]FDG-PET changes in AD using a pipeline to integrate omics with PET imaging data. More specifically, we observed omics-derived modular associations with brain glucose metabolism in AD-vulnerable regions, with the protein serine/threonine kinase activity-related GO cluster and zinc-finger–related regulatory units being the top hits.

The semantic similarity analysis of the GO biological processes revealed clusters of terms altered in AD that are significantly associated with [^{18}F]FDG-PET imaging. The GO cluster most associated with [^{18}F]FDG-PET metabolism represented serine/threonine protein kinase activity. By adding phosphate groups quickly and dynamically, kinases can coordinate and control complex cellular functions, such as energy production, cell growth, and survival. It is known that protein kinases can lead to the spread of aberrant signaling in AD.[49–51] In this sense, kinases such as Akt, extracellular signal-regulated kinase 1 and 2 (ERK1/2), cAMP-dependent protein kinase (PKA), glycogen synthase kinase-3β (GSK-3β), p70S6 kinase, and cyclin-dependent protein kinases 5 (Cdk5) were found with altered expression or activity in AD.[52–55] The hyperactivation of these kinases can lead to abnormal tau phosphorylation, amyloid production, apoptosis, and neuroinflammation. For instance, an increase in GSK-3β activity was observed in individuals with familial AD mutation of amyloid precursor protein (Swedish751).[50]

Applying a reverse engineering strategy, we identified 10 TFs and their regulatory units potentially acting as master regulators and significantly associated with cerebral glucose metabolism. Our findings showed that brain [^{18}F]FDG-PET imaging associates with TFs related to zinc-finger proteins. Specifically, 7 of the top 10 regulatory units with the most association with [^{18}F]FDG-PET are from the zinc-finger

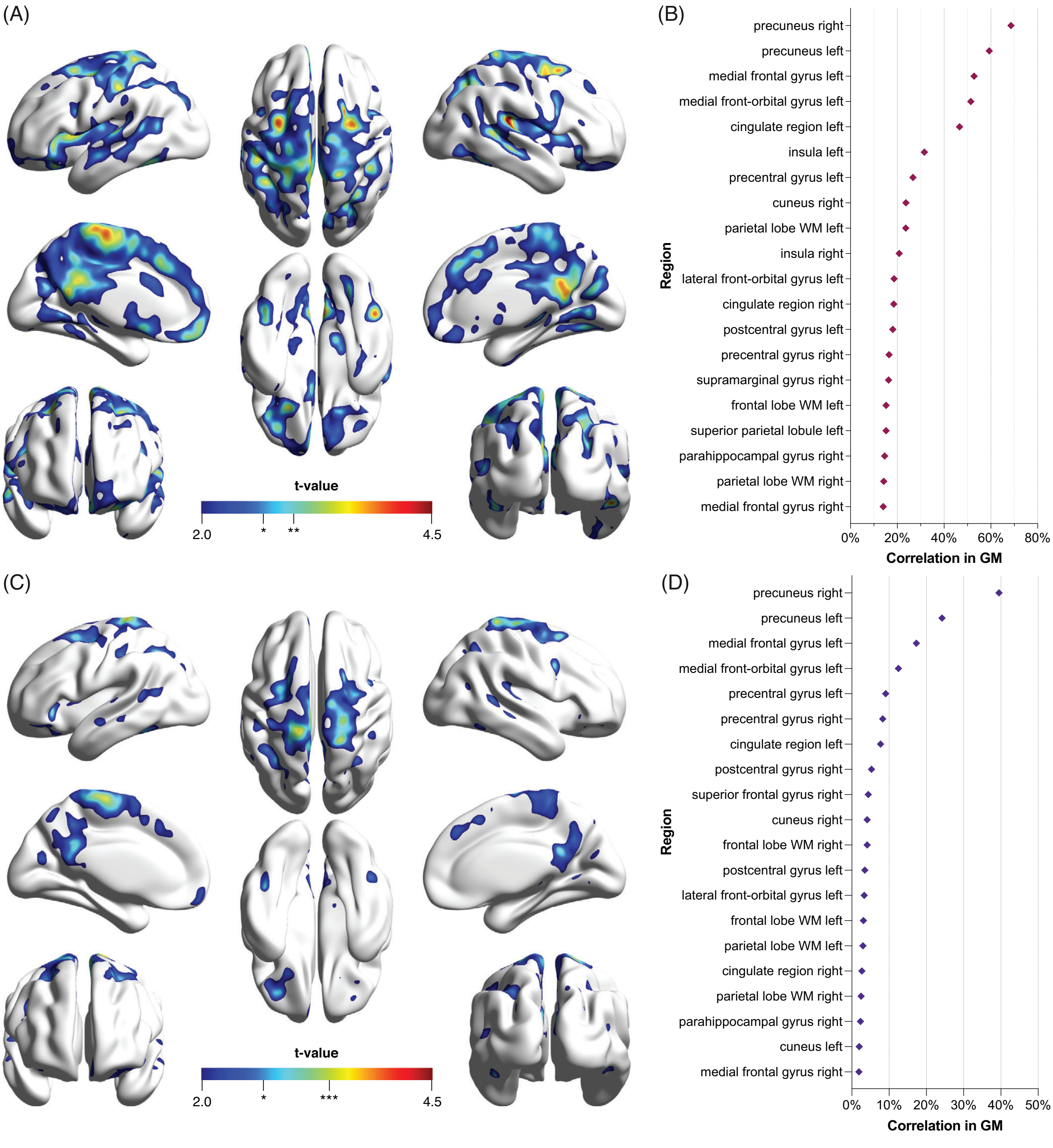

FIGURE 5 Fluorodeoxyglucose positron emission tomography ([^{18}F]FDG-PET) voxel-wise correlations. Voxel-wise correlation between [^{18}F]FDG-PET and the enrichment score of the Gene Ontology (GO) cluster related to the regulation of protein serine/threonine kinase activity (top) and the regulatory unit ZNF653 (bottom). A, C, T-statistical map from the generalized linear regression model. B, D, Top 20 brain regions with more statistically correlated voxels in the gray matter. For the cluster-to-PET integration, peak-$t_{(223)} = 4.86$, P value < 0.001 (right insula). For the ZNF653-to-PET integration, peak-$t_{(223)} = 3.90$, P value < 0.001 (left medial frontal gyrus). value = 2.0, degrees of freedom = 223, P value = 0.05.

family. The zinc-finger units regulate gene expression at the transcriptional and translational levels and are highly expressed in the brain.[56] It has already been demonstrated that zinc-finger genes are associated with pathophysiological changes in AD and regulate the upstream expression of genes related to hyperphosphorylation of tau in AD.[57] This could possibly explain the positive association when integrating [^{18}F]FDG-PET and zinc-finger–related regulatory units enriched with DEGs.

We found no shared GO between the cluster representing serine/threonine protein kinase activity and the top 10 enriched regulatory units. However, the brain regions that showed significant correlations with zinc-finger genes are included in the regions that correlate with the serine/threonine protein kinase activity cluster. This supports the complexity of AD's effects on brain glucose metabolism, suggesting that multiple pathophysiological features are acting independently. Interestingly, the zinc-finger ZNF653 has 52 predicted phosphorylation sites, 9 confirmed in humans, and 5 serine/threonine.[58–60] This way, one could argue that the serine/threonine kinase may be modulating the activity of these TFs. However, while the ZNF653 phosphorylation may be associated with serine/threonine activity, further studies are required to establish a direct link between these phosphorylation events and the regulatory activity of this transcription factor.

A biological definition of AD has recently been proposed solely based on biomarkers.[61] Although it reflects fundamental advances in the development of neuroimaging and fluid biomarkers in AD research, a significant limitation of implementing this framework in clinical practices is the low predictive accuracy of this system.[62] For instance, many amyloid beta (Aβ)- and tau-positive CU individuals remain cognitively stable for their entire lifetime,[62] suggesting that pathophysiological processes beyond Aβ and tau pathologies must be considered.[63] Therefore, it is crucial to enhance our comprehension of the biological features linked to biomarker changes to advance the field. Here, we detected significant biological pathway abnormalities in AD patients, which has the potential to provide insights into AD pathophysiology. Of note, the integration method proposed here is a novel tool that can be applied using multiple PET imaging tracers (e.g., Aβ PET, tau PET, TSPO PET, and others) and adapted in the context of different neurological diseases and omics modalities.

One should note that metabolic disorders and other neurodegenerative conditions may impact [^{18}F]FDG-PET brain metabolism.[64–66] Thus, omics-derived data and brain [^{18}F]FDG-PET integration in other diseases could unveil whether these biological modules are universally associated with brain metabolic changes or whether disease-specific modules exist. Nevertheless, while our study encompassed nine different transcriptomics databases (n = 1170), it is important to note that only one imaging database was used, thereby limiting the breadth of our analysis. Consequently, we acknowledge the necessity of experimental validation of our findings concerning metabolic brain changes in AD.

To conclude, we developed a strategy to integrate modular structures obtained from omics data with PET imaging. We found that a GO cluster related to serine/threonine kinase activity and the regulatory unit related to zinc-finger proteins are highly associated with [^{18}F]FDG-PET in AD. These findings could lead to improved biological interpretation of [^{18}F]FDG-PET imaging and aid in the identification of new biomarkers or therapeutic targets for AD.

ACKNOWLEDGMENTS

Data collection and sharing for this project were funded by the Alzheimer's Disease Neuroimaging Initiative (ADNI, National Institutes of Health Grant U01 AG024904) and DOD ADNI (Department of Defense award number W81XWH-12-2-0012). ADNI is funded by the National Institute on Aging, the National Institute of Biomedical Imaging and Bioengineering, and through generous contributions from the following: AbbVie; Alzheimer's Association; Alzheimer's Drug Discovery Foundation; Araclon Biotech; BioClinica, Inc.; Biogen; Bristol-Myers Squibb Company; CereSpir, Inc.; Cogstate; Eisai, Inc.; Elan Pharmaceuticals, Inc.; Eli Lilly and Company; EuroImmun; F. Hoffmann-La Roche Ltd and its affiliated company Genentech, Inc.; Fujirebio; GE Healthcare; IXICO Ltd.; Janssen Alzheimer Immunotherapy Research & Development, LLC; Johnson & Johnson Pharmaceutical Research & Development LLC; Lumosity; Lundbeck; Merck & Co., Inc.; Meso Scale Diagnostics, LLC; NeuroRx Research; Neurotrack Technologies; Novartis Pharmaceuticals Corporation; Pfizer Inc.; Piramal Imaging; Servier; Takeda Pharmaceutical Company; and Transition Therapeutics. The Canadian Institutes of Health Research is providing funds to support ADNI clinical sites in Canada. Private sector contributions are facilitated by the Foundation for the National Institutes of Health (www.fnih.org). The grantee organization is the Northern California Institute for Research and Education, and the study is coordinated by the Alzheimer's Therapeutic Research Institute at the University of Southern California. ADNI data are disseminated by the Laboratory for NeuroImaging at the University of Southern California. Guilherme Povala receives financial support from the Alzheimer's Association (#24AARFD-1243899). Marco Antônio De Bastiani receives support from CNPq (#150512/2022-8) and the Alzheimer's Association (#AARFD-23-1148735). Bruna Bellaver receives support from the Alzheimer's Association (#AARFD-22-974627). Pamela C. L. Ferreira receives support from the Alzheimer's Association (#AARFD-22-974627). Pedro Rosa-Neto is supported by the Weston Brain Institute, Canadian Institutes of Health Research (#MOP-11-51-31; RFN 152985, 159815, 162303), Canadian Consortium of Neurodegeneration and Aging (MOP-11-51-31-team 1), the Alzheimer's Association (#NIRG-12-92090, #NIRP-12-259245), Brain Canada Foundation (CFI Project 34874 33397), and the Fonds de Recherche du Québec – Santé (Chercheur Boursier, #2020-VICO-279314). Tharick A. Pascoal is supported by the National Institute on Aging (R01AG075336, R01AG073267). João Pedro Ferrari-Souza receives support from CAPES (#88887.627297/2021-00). Eduardo R. Zimmer is supported by CNPq (435642/2018-9; 312410/2018-2; 409066/2022-2; 312306/2021-0; 409595/2023-3), Instituto Serrapilheira (Serra-1912-31365), Brazilian National Institute of Science and Technology in Excitotoxicity and Neuroprotection (465671/2014-4), ARD/FAPERGS (21/2551-0000673-0), Alzheimer's Association and

Natinal Academy of Neuropsychology (ALZ-NAN-22-928381) and the Alzheimer's Association (AARGD-21-850670).

CONFLICT OF INTEREST STATEMENT

Pedro Rosa-Neto has served on the scientific advisory boards of Novo Nordisk, Eisai, and Ely Lilly. He has also served as a consultant to Eisai and Cerveau radiopharmaceuticals. Eduardo R. Zimmer has served on the scientific advisory board of Nintx, Novo Nordisk, and Masima. He is also a co-founder and a minority shareholder at Masima. Marco Antônio De Bastiani is a co-founder and a shareholder at Masima. The other authors have no competing interests to declare. The ADNI study was approved by the institutional review boards of all participating institutions and informed written consent was obtained from all participants at each site. All datasets used in this article are publicly available in the referenced repositories. Further information will be readily available upon request. Author disclosures are available in the supporting information.

DATA AVAILABILITY STATEMENT

Datasets used in this study can be accessed via NCBI GEO (https://www.ncbi.nlm.nih.gov/geo/) and ADNI (https://adni.loni.usc.edu/) portals. Further intermediate data and codes generated are available from the corresponding author upon request.

CONSENT STATEMENT

Consent was not necessary because this study uses online public resources.

REFERENCES

1. Gustavsson A, Norton N, Fast T, et al. Global estimates on the number of persons across the Alzheimer's disease continuum. *Alzheimers Dement*. 2023;19(2):658-670. doi: 10.1002/alz.12694
2. Hane FT, Robinson M, Lee BY, Bai O, Leonenko Z, Albert MS. Recent progress in Alzheimer's disease research, part 3: diagnosis and treatment. *J Alzheimers Dis*. 2016;57:645-665. doi:10.3233/JAD-160907
3. Chételat G, Arbizu J, Barthel H, et al. Amyloid-PET and 18F-FDG-PET in the diagnostic investigation of Alzheimer's disease and other dementias. *Lancet Neurol*. 2020;19:951-962. doi:10.1016/S1474-4422(20)30314-8
4. Zimmer ER, Parent MJ, Souza DG, et al. [18F]FDG PET signal is driven by astroglial glutamate transport. *Nat Neurosci*. 2017;20:393-395. doi:10.1038/nn.4492
5. Wang H-F, Tan L, Cao L, et al. Application of the IWG-2 diagnostic criteria for Alzheimer's disease to the ADNI. *J Alzheimers Dis*. 2016;51:227-236. doi:10.3233/JAD-150824
6. Zimmer ER, Pascoal TA, Rosa-Neto P, Nordberg A, Pellerin L. Comment on ''Microglial activation states drive glucose uptake and FDG-PET alterations in neurodegenerative diseases. *Sci Transl Med*. 2022;14:eabm8302. doi:10.1126/scitranslmed.abm8302
7. Xiang X, Wind K, Wiedemann T, et al. Microglial activation states drive glucose uptake and FDG-PET alterations in neurodegenerative diseases. *Sci Transl Med*. 2021;13:eabe5640. doi:10.1126/scitranslmed.abe5640
8. Rocha A, Bellaver B, Souza DG, et al. Clozapine induces astrocyte-dependent FDG-PET hypometabolism. *Eur J Nucl Med Mol Imaging*. 2022;49:2251-2264. doi:10.1007/s00259-022-05682-3
9. Sala A, Lizarraga A, Caminiti SP, et al. Brain connectomics: time for a molecular imaging perspective? *Trends Cogn Sci*. 2023;27:353-366. doi:10.1016/j.tics.2022.11.015
10. Chan YH, Wang C, Soh WK, Rajapakse JC. Combining neuroimaging and omics datasets for disease classification using graph neural networks. *Front Neurosci*. 2022;16:1-15. doi:10.3389/fnins.2022.866666
11. Verheijen J, Sleegers K. Understanding Alzheimer disease at the interface between genetics and transcriptomics. *Trends Genet TIG*. 2018;34:434-447. doi:10.1016/j.tig.2018.02.007
12. Villoslada P, Steinman L, Baranzini SE. Systems biology and its application to the understanding of neurological diseases. *Ann Neurol*. 2009;65:124-139. doi:10.1002/ana.21634
13. Iturria-Medina Y, Carbonell F, Assadi A, et al. Integrating molecular, histopathological, neuroimaging and clinical neuroscience data with NeuroPM-box. *Commun Biol*. 2021;4:1-20. doi:10.1038/s42003-021-02133-x
14. Zeiler FA, Iturria-Medina Y, Thelin EP, et al. Integrative neuroinformatics for precision prognostication and personalized therapeutics in moderate and severe traumatic brain injury. *Front Neurol*. 2021;12:729184. doi:10.3389/fneur.2021.729184
15. Petersen RC, Aisen PS, Beckett LA, et al. Alzheimer's disease neuroimaging initiative (ADNI): clinical characterization. *Neurology*. 2010;74:201-209. doi:10.1212/WNL.0b013e3181cb3e25
16. Alzheimer's Disease Neuroimaging Initiative (ADNI). ADNI General Procedures Manual. 2024 Retrieved from https://adni.loni.usc.edu/wp-content/uploads/2024/02/ADNI_General_Procedures_Manual_29Feb2024.pdf
17. Davis S, Meltzer PS. GEOquery: a bridge between the Gene Expression Omnibus (GEO) and BioConductor. *Bioinforma Oxf Engl*. 2007;23:1846-1847. doi:10.1093/bioinformatics/btm254
18. Sood S, Gallagher IJ, Lunnon K, et al. A novel multi-tissue RNA diagnostic of healthy ageing relates to cognitive health status. *Genome Biol*. 2015;16:185. doi:10.1186/s13059-015-0750-x
19. Naughton BJ, Duncan FJ, Murrey DA, et al. Blood genome-wide transcriptional profiles reflect broad molecular impairments and strong blood-brain links in Alzheimer's disease. *J Alzheimers Dis JAD*. 2015;43:93-108. doi:10.3233/JAD-140606
20. Westra H-J, Peters MJ, Esko T, et al. Systematic identification of trans eQTLs as putative drivers of known disease associations. *Nat Genet*. 2013;45:1238-1243. doi:10.1038/ng.2756
21. Shamir R, Klein C, Amar D, et al. Analysis of blood-based gene expression in idiopathic Parkinson disease. *Neurology*. 2017;89:1676-1683. doi:10.1212/WNL.0000000000004516
22. Heider A, Alt R. virtualArray: a R/bioconductor package to merge raw data from different microarray platforms. *BMC Bioinf*. 2013;14:75. doi:10.1186/1471-2105-14-75
23. Liang WS, Dunckley T, Beach TG, et al. Gene expression profiles in anatomically and functionally distinct regions of the normal aged human brain. *Physiol Genomics*. 2007;28:311-322. doi:10.1152/physiolgenomics.00208.2006
24. Blalock EM, Buechel HM, Popovic J, Geddes JW, Landfield PW. Microarray analyses of laser-captured hippocampus reveal distinct gray and white matter signatures associated with incipient Alzheimer's disease. *J Chem Neuroanat*. 2011;42:118-126. doi:10.1016/j.jchemneu.2011.06.007
25. Miller JA, Woltjer RL, Goodenbour JM, Horvath S, Geschwind DH. Genes and pathways underlying regional and cell type changes in Alzheimer's disease. *Genome Med*. 2013;5:48. doi:10.1186/gm452
26. Hokama M, Oka S, Leon J, et al. Altered expression of diabetes-related genes in Alzheimer's disease brains: the Hisayama study. *Cereb Cortex*. 2014;24:2476-2488. 1991. doi:10.1093/cercor/bht101
27. Berchtold NC, Cribbs DH, Coleman PD, et al. Gene expression changes in the course of normal brain aging are sexually dimorphic.

Proc Natl Acad Sci USA. 2008;105:15605-15610. doi:10.1073/pnas.0806883105
28. Wang M, Roussos P, McKenzie A, et al. Integrative network analysis of nineteen brain regions identifies molecular signatures and networks underlying selective regional vulnerability to Alzheimer's disease. *Genome Med*. 2016;8:104. doi:10.1186/s13073-016-0355-3
29. Gautier L, Cope L, Bolstad BM, Irizarry RA. affy–analysis of Affymetrix GeneChip data at the probe level. *Bioinforma Oxf Engl*. 2004;20:307-315. doi:10.1093/bioinformatics/btg405
30. Huber W, von Heydebreck A, Sültmann H, Poustka A, Vingron M. Variance stabilization applied to microarray data calibration and to the quantification of differential expression. *Bioinforma Oxf Engl*. 2002;18(Suppl 1):S96-104. doi:10.1093/bioinformatics/18.suppl_1.s96
31. Leek JT, Johnson WE, Parker HS, Jaffe AE, Storey JD. The sva package for removing batch effects and other unwanted variation in high-throughput experiments. *Bioinforma Oxf Engl*. 2012;28:882-883. doi:10.1093/bioinformatics/bts034
32. Ritchie ME, Phipson B, Wu D, et al. limma powers differential expression analyses for RNA-sequencing and microarray studies. *Nucleic Acids Res*. 2015;43:e47. doi:10.1093/nar/gkv007
33. Chen H, Boutros PC. VennDiagram: a package for the generation of highly-customizable Venn and Euler diagrams in R. *BMC Bioinf*. 2011;12:35. doi:10.1186/1471-2105-12-35
34. Yu G, Wang L-G, Han Y, He Q-Y. clusterProfiler: an R package for comparing biological themes among gene clusters. *OMICS J Integr Biol*. 2012;16:284-287. doi:10.1089/omi.2011.0118
35. Yu G, Li F, Qin Y, Bo X, Wu Y, Wang S. GOSemSim: an R package for measuring semantic similarity among GO terms and gene products. *Bioinforma Oxf Engl*. 2010;26:976-978. doi:10.1093/bioinformatics/btq064
36. Castro MA, Wang X, Fletcher MN, Meyer KB, Markowetz F. RedeR: R/Bioconductor package for representing modular structures, nested networks and multiple levels of hierarchical associations. *Genome Biol*. 2012;13:R29. doi:10.1186/gb-2012-13-4-r29
37. Castro MAA, de Santiago I, Campbell TM, et al. Regulators of genetic risk of breast cancer identified by integrative network analysis. *Nat Genet*. 2016;48:12-21. doi:10.1038/ng.3458
38. Fletcher MNC, Castro MAA, Wang X, et al. Master regulators of FGFR2 signalling and breast cancer risk. *Nat Commun*. 2013;4:2464. doi:10.1038/ncomms3464
39. Margolin AA, Wang K, Lim WK, Kustagi M, Nemenman I, Califano A. Reverse engineering cellular networks. *Nat Protoc*. 2006;1:662-671. doi:10.1038/nprot.2006.106
40. Lambert SA, Jolma A, Campitelli LF, et al. The human transcription factors. *Cell*. 2018;172:650-665. doi:10.1016/j.cell.2018.01.029
41. Kin Chan SS. What is a master regulator? *J Stem Cell Res Ther*. 2013;03:1-2. doi:10.4172/2157-7633.1000e114
42. Margolin AA, Nemenman I, Basso K, et al. ARACNE: an algorithm for the reconstruction of gene regulatory networks in a mammalian cellular context. *BMC Bioinf*. 2006;7:S7. doi:10.1186/1471-2105-7-S1-S7
43. Carro MS, Lim WK, Alvarez MJ, et al. The transcriptional network for mesenchymal transformation of brain tumours. *Nature*. 2010;463:318-325. doi:10.1038/nature08712
44. Hänzelmann S, Castelo R, Guinney J. GSVA: gene set variation analysis for microarray and RNA-Seq data. *BMC Bioinf*. 2013;14:7. doi:10.1186/1471-2105-14-7
45. Avants BB, Tustison NJ, Stauffer M, Song G, Wu B, Gee JC. The Insight ToolKit image registration framework. *Front Neuroinform*. 2014;8:1-13. doi:10.3389/fninf.2014.00044
46. Lerch J, Hammill C, van Eede M, Cassel D. RMINC: Statistical Tools for Medical Imaging NetCDF (MINC) Files. R package version 1.5.2.1. 2017. http://mouse-imaging-centre.github.io/RMINC
47. Manera AL, Dadar M, Fonov V, Collins DL. CerebrA, registration and manual label correction of Mindboggle-101 atlas for MNI-ICBM152 template. *Sci Data*. 2020;7(1). doi:10.1038/s41597-020-0557-9
48. Klein A, Tourville J. 101 labeled brain images and a consistent human cortical labeling protocol. *Front Neurosci*. 2012;6:171. doi:10.3389/fnins.2012.00171
49. Perluigi M, Barone E, Di Domenico F, Butterfield DA. Aberrant protein phosphorylation in Alzheimer disease brain disturbs pro-survival and cell death pathways. *Biochim Biophys Acta*. 2016;1862:1871-1882. doi:10.1016/j.bbadis.2016.07.005
50. Ryder J, Su Y, Ni B. Akt/GSK3beta serine/threonine kinases: evidence for a signalling pathway mediated by familial Alzheimer's disease mutations. *Cell Signal*. 2004;16:187-200. doi:10.1016/j.cellsig.2003.07.004
51. Rosenberger AFN, Hilhorst R, Coart E, et al. Protein kinase activity decreases with higher Braak stages of Alzheimer's disease pathology. *J Alzheimers Dis JAD*. 2016;49:927-943. doi:10.3233/JAD-150429
52. Hodges SL, Reynolds CD, Smith GD, Jefferson TS, Nolan SO, Lugo JN. Molecular interplay between hyperactive mammalian target of rapamycin signaling and Alzheimer's disease neuropathology in the NS-Pten knockout mouse model. *Neuroreport*. 2018;29:1109-1113. doi:10.1097/WNR.0000000000001081
53. Griffin RJ, Moloney A, Kelliher M, et al. Activation of Akt/PKB, increased phosphorylation of Akt substrates and loss and altered distribution of Akt and PTEN are features of Alzheimer's disease pathology. *J Neurochem*. 2005;93:105-117. doi:10.1111/j.1471-4159.2004.02949.x
54. Liu H, Jin X, Yin X, Jin N, Liu F, Qian W. PKA-CREB signaling suppresses tau transcription. *J Alzheimers Dis JAD*. 2015;46:239-248. doi:10.3233/JAD-142610
55. Maitra S, Vincent B. Cdk5-p25 as a key element linking amyloid and tau pathologies in Alzheimer's disease: mechanisms and possible therapeutic interventions. *Life Sci*. 2022;308:120986. doi:10.1016/j.lfs.2022.120986
56. ZNF653 zinc finger protein 653 [Homo sapiens (human)]—Gene—NCBI. n.d. Accessed April 25, 2022. https://www.ncbi.nlm.nih.gov/gene?Db=gene&Cmd=DetailsSearch&Term=115950#gene-expression
57. Bu S, Lv Y, Liu Y, Qiao S, Wang H. Zinc finger proteins in neuro-related diseases progression. *Front Neurosci*. 2021;15:760567. doi:10.3389/fnins.2021.760567
58. Kinexus | PhosphoNET. n.d. Accessed September 30, 2022. http://www.phosphonet.ca/?search=Q96CK0
59. Becnel LB, Darlington YF, Ochsner SA, et al. Nuclear receptor signaling Atlas: opening access to the biology of nuclear receptor signaling pathways. *PLoS One*. 2015;10:e0135615. doi:10.1371/journal.pone.0135615
60. Borud B, Mellgren G, Lund J, Bakke M. Cloning and characterization of a novel zinc finger protein that modulates the transcriptional activity of nuclear receptors. *Mol Endocrinol*. 2003;17:2303-2319. doi:10.1210/me.2003-0158
61. Jack CR, Bennett DA, Blennow K, et al. NIA-AA research framework: toward a biological definition of Alzheimer's disease. *Alzheimers Dement*. 2018;14:535-562. doi:10.1016/j.jalz.2018.02.018
62. Dubois B, Villain N, Frisoni GB, et al. Clinical diagnosis of Alzheimer's disease: recommendations of the International Working Group. *Lancet Neurol*. 2021;20:484-496. doi:10.1016/S1474-4422(21)00066-1
63. Ossenkoppele R, Pichet Binette A, Groot C, et al. Amyloid and tau PET-positive cognitively unimpaired individuals are at high risk for future cognitive decline. *Nat Med*. 2022;28:2381-2387. doi:10.1038/s41591-022-02049-x
64. Grimmer T, Diehl J, Drzezga A, Förstl H, Kurz A. Region-specific decline of cerebral glucose metabolism in patients with frontotemporal dementia: a prospective ^{18}F-FDG-PET study. *Dement Geriatr Cogn Disord*. 2004;18:32-36. doi:10.1159/000077732

Alzheimer's & Dementia®
THE JOURNAL OF THE ALZHEIMER'S ASSOCIATION

65. Whitwell JL, Graff-Radford J, Singh TD, et al. ^{18}F-FDG PET in posterior cortical atrophy and dementia with Lewy bodies. *J Nucl Med*. 2017;58:632-638. doi:10.2967/jnumed.116.179903
66. Minoshima S, Foster NL, Sima AAF, Frey KA, Albin RL, Kuhl DE. Alzheimer's disease versus dementia with Lewy bodies: cerebral metabolic distinction with autopsy confirmation. *Ann Neurol*. 2001;50:358-365. doi:10.1002/ana.1133

SUPPORTING INFORMATION

Additional supporting information can be found online in the Supporting Information section at the end of this article.

How to cite this article: Povala G, De Bastiani MA, Bellaver B, et al. Omics-derived biological modules reflect metabolic brain changes in Alzheimer's disease. *Alzheimer's Dement*. 2024;1-13. https://doi.org/10.1002/alz.14095